EARTHQUAKE ENGINEERING AND STRUCTURAL DYNAMICS
Earthquake Engng. Struct. Dyn. **27**, 1483–1502 (1998)

THREE-DIMENSIONAL NON-LINEAR SOIL–BUILDING INTERACTION ANALYSIS IN THE LAKEBED ZONE OF MEXICO CITY DURING THE HYPOTHETICAL GUERRERO EARTHQUAKE

MASAHIRO IIDA*
Earthquake Research Institute, University of Tokyo, Tokyo, Japan

SUMMARY

The 1985 Michoacan earthquake ($M = 8{\cdot}1$) caused very severe damage to mid-rise buildings in the lakebed zone of Mexico City, which is approximately 400 km from the epicentre in the Pacific Ocean. In the present study, we perform a three-dimensional (3-D) non-linear soil–building interaction analysis for several types of low- to high-rise buildings during the hypothetical Guerrero earthquake, and try to understand the real cause of heavy damage to mid-rise buildings in the lakebed zone during the 1985 Michoacan earthquake. We make a reasonable estimation of the input earthquake motions and the local site effects. The non-linear soil-building interaction analysis explains the damage pattern observed during the 1985 earthquake, although other analyses do not. We realize that all the factors from the earthquake source to the building superstructure must be taken into account adequately. © 1998 John Wiley & Sons, Ltd.

KEY WORDS: 3-D non-linear response analysis; soil–building interaction; lakebed zone; Mexico City; hypothetical Guerrero earthquake

1. INTRODUCTION

The 19 September 1985 Michoacan earthquake ($M = 8{\cdot}1$) caused very severe damage in Mexico City inside the Valley of Mexico, which is approximately 400 km from the epicentre in the Pacific Ocean. The Valley of Mexico is divided into the three geological zones: the hill zone, the transition zone, and the lakebed zone. Whereas the earthquake produced very low accelerations at epicentral stations, seismic waves were amazingly amplified inside the valley, especially in the lakebed zone, and the long duration of the lakebed seismograms was a real surprise.

In some areas of the lakebed zone of Mexico City, the very heavy damage to mid-rise (7–15-storey) buildings was quite impressive, in spite of the light damage to low-rise and high-rise buildings, and other structures. The predominant periods of ground surface in disastrous areas lay in the range of 1·5–2·5 s.[1]

In order to understand the real cause of the heavy damage to buildings, we must estimate input earthquake motions, local site effects, and soil–building interaction effects. Soil–building interaction effects are expected to be very noticeable in the case of large-scale structures constructed on soft-soil ground.

* Correspondence to: Masahiro Iida, Earthquake Research Institute, University of Tokyo, 1-1-1 Yayoi, Bunkyo-ku, Tokyo 113-0032, Japan. E-mail: iida@eri.u-tokyo.ac.jp

Contract/grant sponsor: Ministry of Education, Japan
Contract/grant sponsor: Kajima Foundation

CCC 0098–8847/98/121483–20$17·50

Received 27 May 1997
Revised 28 October 1997 and 9 April 1998

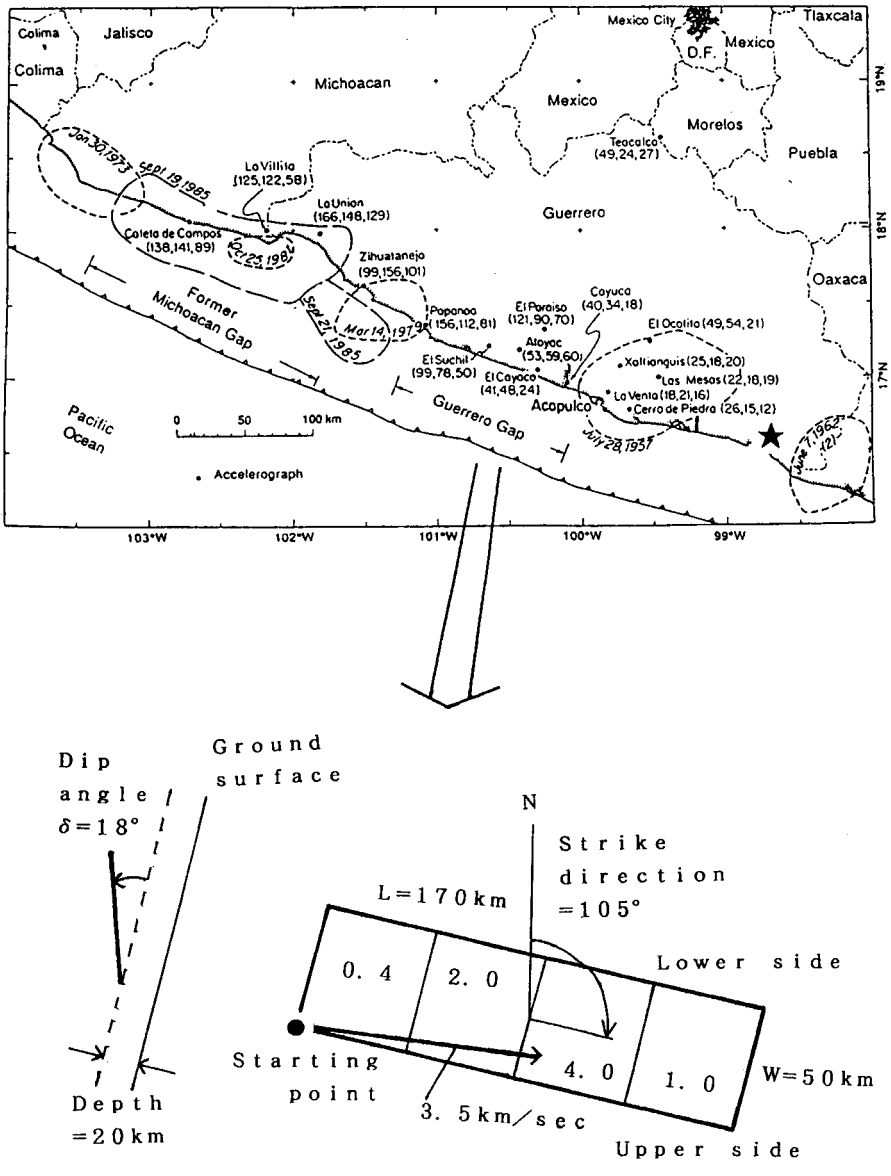

Figure 1. Map of coastal Mexico, indicating aftershock zones of large earthquakes since 1951 (after Anderson *et al.*[2]) and modelling of the hypothetical Guerrero earthquake. The fault plane is 170 km × 50 km, with a strike direction of 105° and a dip angle of 18°. The upper edge of the fault area is at a depth of about 20 km. The fault rupture velocity is 3·5 km/s. Numerical values on the fault plane indicate the seismic moment ratio of the fault element to the 14 September 1995 earthquake. The S-wave propagation velocity is 4.0 km/s, with a quality factor Q of 500 (an attenuation constant of 0.001) for S waves. The epicentre of the 1995 earthquake is shown by a star

In the present study, we perform a 3-D non-linear soil-building interaction analysis for several types of low-rise to high-rise buildings in the lakebed zone of Mexico City during the hypothetical Guerrero earthquake ($M = 8{\cdot}1$), and try to understand the real cause of heavy damage to mid-rise buildings in the lakebed zone during the 1985 Michoacan earthquake. We are more curious about the building behaviour during the anticipated Guerrero earthquake rather than that during previous earthquakes. At the same time,

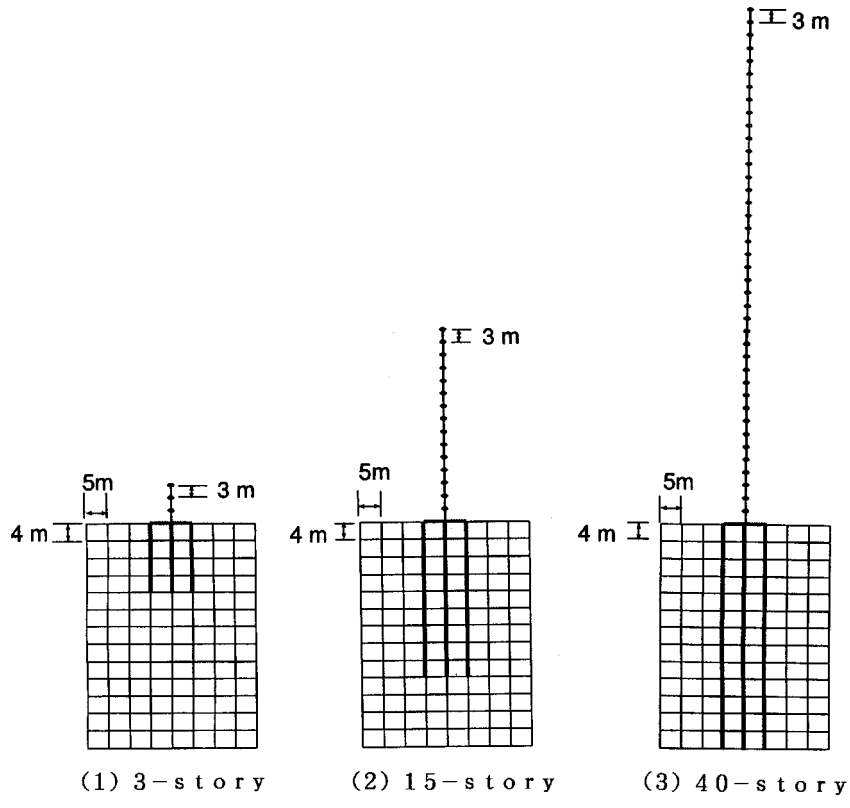

Figure 2. Three-dimensional building–foundation–pile–soil system. Five building models are used in the interaction analyses and only three of them are shown here

the validity of the approach is demonstrated by comparing the calculated building behaviour with the building behaviour observed during the 1985 Michoacan earthquake. The anticipated Guerrero earthquake is equivalent to the 1985 Michoacan earthquake in earthquake magnitude and mechanism (Figure 1), so we can expect damage patterns for both the earthquakes to be practically similar. No complete response analyses have been conducted in Mexico with an exception of a 2-D linear soil–building interaction analysis done by Romo.[3]

2. METHODOLOGY

We use a 3-D model only for the upper volume (Figure 2) and a 1-D model for the lower volume. Soil–building interaction effects are considered by using a 3-D soil-building interaction system based upon the finite element method. The depth of the bottom plane of the 1-D modelled volume is equal to a depth of an underground instrument at a borehole strong-motion station where the shallow underground profile has been surveyed, and strong-motion excitation as shear waves is applied at this depth. Therefore, a summation method of semi-empirical Green's functions is employed at the depth of the underground instrument in order to obtain strong-motion accelerograms for large earthquakes. One-dimensional propagation of vertically incident S waves is used in the 1-D modelled volume. The upcoming waves are input to the bottom plane of the 3-D modelled volume.

2.1. Methods for analysing soil–building interaction

We perform a 3-D seismic non-linear soil–building interaction analysis based upon the finite element method. The analysis was developed by Ishihara and Miura.[4] There are only a few 3-D non-linear response analyses.[5–7] Our building–foundation–pile–soil system is shown in Figure 2. The building superstructure rests on a rigid box foundation supported on piles. Each pile is modelled by beam elements, and the soil volume by 3-D rectangular prism elements.

The equation of motion which connects the building superstructure, the rigid foundation, the frictional piles, and the soil is derived. Since the foundation is rigid, the matrix representing the contribution of the superstructure in the equation of motion becomes a general matrix in the case of the fixed foundation. The seismic motion at a point which is sufficiently far away from the building is assumed to be equal to the free-field motion, because effects of soil–building interaction can be ignored. Therefore, we can apply the free-field motion as the seismic motion at the boundary of the analytical model. This leads to a reduction of the 3-D volume which needs to be modelled.

The final equation of motion is represented by the following two equations:

$$\begin{bmatrix} M_{aa} & M_{ab} & 0 \\ M_{ba} & M_{bb} & M_{bc} \\ 0 & M_{cb} & M_{cc} \end{bmatrix} \begin{Bmatrix} \ddot{\delta}_a + \ddot{\delta}_g \\ \ddot{\delta}_b + \ddot{\delta}_g \\ \ddot{\delta}_c + \ddot{\delta}_g \end{Bmatrix} + \begin{bmatrix} C_{aa} & C_{ab} & 0 \\ C_{ba} & C_{bb} & C_{bc} \\ 0 & C_{cb} & C_{cc} \end{bmatrix} \begin{Bmatrix} \dot{\delta}_a \\ \dot{\delta}_b \\ \dot{\delta}_c \end{Bmatrix} + \begin{bmatrix} K_{aa} & K_{ab} & 0 \\ K_{ba} & K_{bb} & K_{bc} \\ 0 & K_{cb} & K_{cc} \end{bmatrix} \begin{Bmatrix} \delta_a \\ \delta_b \\ \delta_c \end{Bmatrix} = \begin{Bmatrix} P_a \\ P_b \\ P_{cd} \end{Bmatrix}$$

$$P_{cd} = P_c - M_{cd}(\ddot{\delta}_d + \ddot{\delta}_g) - C_{cd}\dot{\delta}_d - K_{cd}\delta_d$$

M, C, K, δ, and P are the mass matrix, the damping matrix, the stiffness matrix, the displacement vector, and the external force vector, respectively. Subscripts a, b, c, d, and g correspond to the building superstructure, the rigid foundation, the frictional piles or the soil deposits, the boundary of the upper 3-D modelled volume, and the bottom plane of the lower 1-D modelled volume, respectively.

We simultaneously model the material non-linearity of the building superstructure, the pile foundation, and the soil. At first, a bilinear model and a yield shear strength are assumed for the building superstructure. Second, we use a criterion that the pile yield strength depends upon the axial force and the bending moment. We set joint elements at both edges of each beam element used to model the pile, in order to consider the slip between the pile and the soil. Third, a bilinear model and the Mohr–Coulomb criterion are assumed for the soil. Also, prior to the main dynamic simulation, initial stresses produced by ground subsidence are evaluated. The ground-subsidence simulation is performed as a static non-linear soil-building interaction analysis under the action of gravity assuming a fixed boundary condition of the bottom plane of the upper 3-D modelled volume. The non-linear equation of motion is solved by the Newton–Raphson method.

Some important parameters were determined by preliminary numerical simulations. These parameters are (1) the damping coefficient for the soil, (2) the horizontal extention of the volume to be modelled, and (3) the calculation time interval. The damping coefficient is important in order to attenuate reflected waves generated at the boundary of the analytical model.

2.2. Methods for estimating input earthquake motions

We use a semi-empirical Green's function summation method to simulate earthquake motions at a depth of an underground instrument at a borehole strong-motion station. Using a semi-empirical method, effects of the earthquake source, the long path from the Pacific Ocean to the Valley of Mexico, the Valley of Mexico

itself, and the soft surficial layers in the lakebed zone, can be incorporated. There are a lot of semi-empirical Green's function summation methods,[8–13] but so far no one has used any of them at subsurface locations such as the location of an underground instrument of a borehole station. Although strong motions might be affected by non-linear behaviour of soil near the ground surface, they are independent of soil non-linearity at deeper layers, so that synthesis of underground accelerograms is, in fact, quite reasonable.

The synthetic method used in this study was developed by Iida and Hakuno.[13] In their method, the synthetic S-wave accelerogram $F(t)$ is represented by the following equation:

$$F(t) = \sum_{e=1}^{X} G_e(t) * H_e * E(t - s_e/V_r - r_e/V_s)$$

where X is the total number of fault elements, E is the accelerogram recorded during a small earthquake, s is the distance between the starting point of the fault rupture and the centre of a fault element, V_r is the fault rupture velocity, r is the distance between the centre of a fault element and the borehole station, V_s is the S-wave propagation velocity, G is the function for the hypocentral distance correction, H is the constant for the seismic moment correction (the seismic moment $M_0 = \mu DS$, where μ is the rigidity, D is the dislocation, and S is the fault area), $*$ is the convolution operator, t is the time, and subscript e indicates the eth fault element.

The source parameters of the hypothetical Guerrero earthquake are displayed in Figure 1. A non-uniform distribution of seismic moment on the fault area is assumed, because a large earthquake is generally composed of multiple events with different seismic moments. The fault rupture velocity is assumed to be constant with the wave front concentric at the starting point of rupture. The differences in the fault mechanism (strike direction, dip angle, etc.) and the station direction between the hypothetical large earthquake and a small one used in the synthesis are ignored. Owing to the difference in the hypocentre location between the two earthquakes, the amplitude of the recorded accelerogram is modified considering the internal damping.

3. ROMA-C BOREHOLE STRONG-MOTION STATION

The underground profile in the lakebed zone of Mexico City is primarily characterized by very low S-wave velocity and extremely low density, around 1·0 g/cm^3, in the upper 50 m. Large non-linear behaviour of the soil is not expected, because the main surface material is high-strength clay. Small non-linear behaviour of the soil was recognized in an analysis of strong-motion records at only one station during the 1985 Michoacan earthquake.[14]

We select the Roma-C borehole strong-motion station operated by the National Disaster Prevention Center of Mexico, in the lakebed zone. The station is located in an area where heavy damage occurred during the 1985 Michoacan earthquake of $M = 8{\cdot}1$. At this borehole station, there are a surface instrument, and two underground instruments at depths of 30 and 102 m. All three strong-motion instruments record three components. Strong-motion accelerograms are synthesized at the depth of 102 m. Figure 3 shows the underground profile at the Roma-C borehole station. The upper 44 m layers are composed of clay, while the lower layers are of sand. In particular, the uppermost 33 m layers are extremely soft. This stratigraphy is typical of the underground profile in the lakebed zone. The primary predominant period calculated from the underground profile is about 2·5 s.

As the Green's function, we use accelerograms obtained at the depth of 102 m during the $M = 7{\cdot}3$ 14 September 1995 earthquake, which occurred in the state of Guerrero (Figure 1). These accelerograms are one of the best-quality records ever obtained in Mexico. Unfortunately, we have no good records at this station from an earthquake in the Michoacan epicentral region, and no borehole seismograms were recorded during the 1985 Michoacan earthquake. Therefore, we select a simulation for the hypothetical Guerrero earthquake

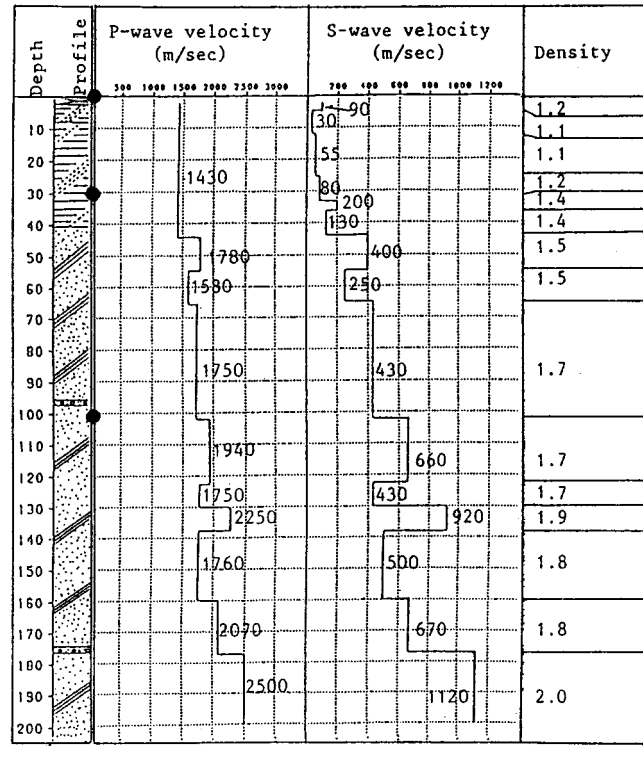

Figure 3. Underground profile at the Roma-C borehole station. Strong-motion instruments are indicated by solid circles

rather than a reproduction of the 1985 Michoacan earthquake. The borehole strong-motion accelerograms are shown in Figure 4. The predominant periods of motion on the ground surface are 2·0–2·5 s while those at the depth of 102 m are ambiguous.

4. THREE-DIMENSIONAL BUILDING RESPONSE ANALYSES

During the 1985 Michoacan earthquake, the fundamental periods of damaged buildings were not consistent with the primary predominant periods of ground surface. This suggests large soil–building interaction effects in the very soft surficial layers. Also, non-linear behaviour of the building superstructure, the pile foundation, and the soil deposits could have played important roles. Besides, ground subsidence might play a significant role in the lakebed zone of Mexico City, since ground subsidence of several-ten centimeters per year is actually recognized.

Consequently, the following four types of analyses are performed:

Analysis (1) = Linear, base-fixed analysis
Analysis (2) = Non-linear, base-fixed analysis
Analysis (3) = Linear, soil–building interaction analysis
Analysis (4) = Non-linear, soil–building interaction analysis

The specific analytical conditions are summarized in Table I. Sway-rocking effects are taken into account in the soil–building interaction analyses. In Analysis (4), initial stresses produced by ground subsidence are also considered.

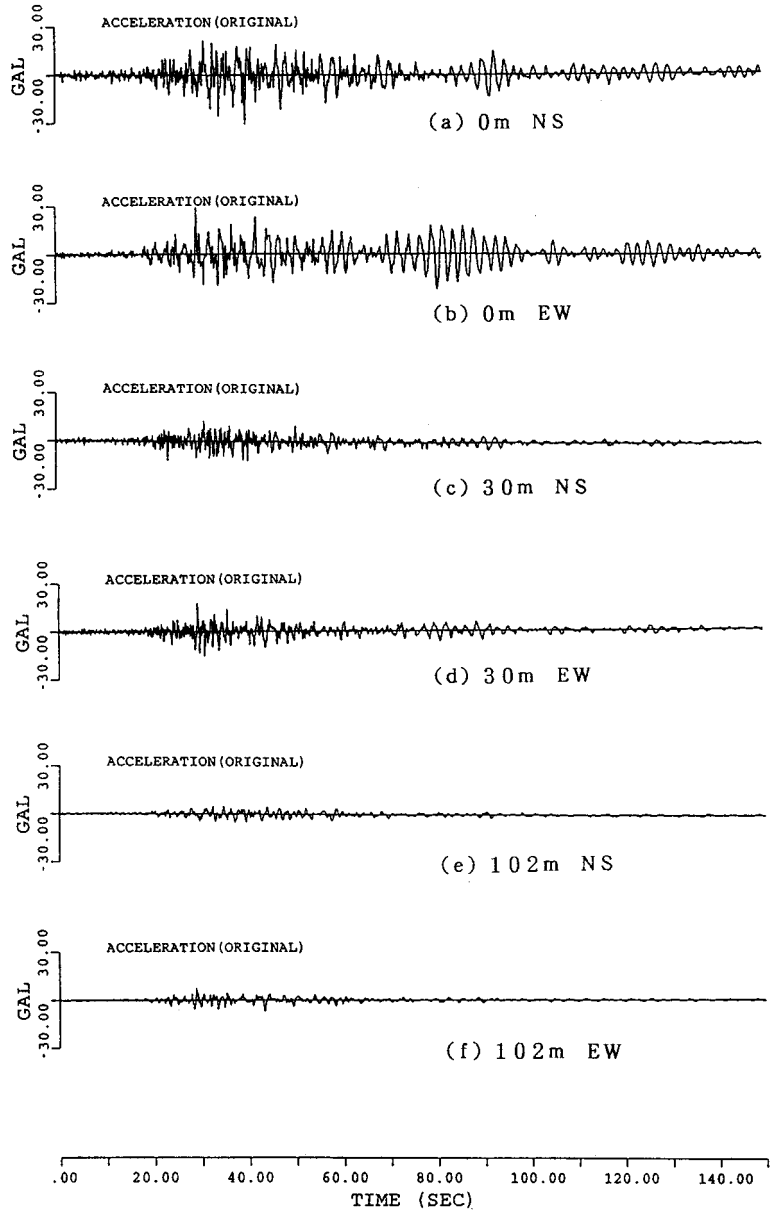

Figure 4. Strong-motion accelerograms (two horizontal components) recorded at the Roma-C borehole station during the 14 September 1995 earthquake

4.1. Building models

In order to understand the observed damage pattern, five standard building models, a low-rise (3-storey), two mid-rise (9-storey and 15-storey), and two high-rise (25-storey and 40-storey) buildings are analyzed. Their fundamental periods derived from a base-fixed condition are shown in Table II. Three examples of the building models used in the interaction analyses are shown in Figure 2. As for the building superstructure, the models for the base-fixed analyses are completely the same as those used in the interaction analyses.

Table I. Analytical conditions for the 4 types of analyses

	Superstructure	Pile	Soil	Ground subsidence
Analysis (1)	Linear	—	Linear*	—
Analysis (2)	Non-linear	—	Linear*	—
Analysis (3)	Linear	Linear	Linear	—
Analysis (4)	Non-linear	Non-linear	Non-linear	Considered

* Means that input surface motions are obtained by a linear assumption of soil behaviour.

Table II. Fundamental periods of the building models

	Fundamental period(s)
(1) 3-storey building	0·41
(2) 9-storey building	0·95
(3) 15-storey building	1·41
(4) 25-storey building	2·04
(5) 40-storey building	2·84

Table III. Assumed length and radii for the piles of the building models

	Length (m)	Radius (m)
(1) 3-storey building	12	0·5
(2) 9-storey building	24	0·9
(3) 15-storey building	36	1·2
(4) 25-storey building	48	1·3
(5) 40-storey building	52	1·5

4.2. Model parameters

As shown in Figure 2, the 3-D model has a horizontal extension of 40 m by 40 m and a vertical extension down to a depth of 52 m. Rectangular prism elements with a base of 5 m × 5 m and a height of 4 m are used to model the soil. A rigid foundation with a horizontal extension of 10 m by 10 m and 9 (3 × 3) piles placed at 5 m intervals are used for all five building models. For the tall building models, one pile is used to model several piles which would be used to support such tall builldings. Each frictional pile is modelled by beam elements with a length of 4 m.

The sizes and weights of the superstructure and the foundation vary from one building model to other. The pile length, size and strength depend upon the building model. The pile length and radii are shown in Table III, and the pile strength is explained in the next subsection. The elastic modulus and density of all piles are $1{\cdot}7 \times 10^6$ and $2{\cdot}3\ (\mathrm{t/m^3})$, respectively. The model parameters are determined by preliminary numerical simulations taking into consideration the CPU time and computer memory required for the calculations.

The damping coefficient for the soil and the calculation time interval are determined as 0·05 and 0·01 s, respectively. The damping coefficient of 0.05 for the soil deposits and the horizontal and vertical extensions of the 3-D model do not produce any confusing wave reflections from the bottom and side walls.

Table IV. Assumed yield shear strength for the 1st and top storeys of the building models

	1st storey (t)	Top storey (t)
(1) 3-storey building	520	440
(2) 9-storey building	760	440
(3) 15-storey building	1060	440
(4) 25-storey building	1400	440
(5) 40-storey building	2000	440

Table V. Assumed yield strength for the piles of the building models

	Tension (t)	Compression (t)	Bending moment (t m)
(1) 3-storey building	270	330	13
(2) 9-storey building	860	1080	43
(3) 15-storey building	1540	1920	77
(4) 25-storey building	1800	2250	90
(5) 40-storey building	4000	5000	200

Table VI. Assumed yield strength for the soil deposits

Depth (m)	Material	Cohesion (t/m^2)	Frictional angle (°)
0–32	Clay	2·5	5
32–44	Clay	3·5	5
44–52	Sand	5·0	30

4.3. Non-linear material parameters

The parameters for the three types of material non-linearity are described. Table IV shows the yield shear strength assumed for the 1st and top storeys. The yield shear strength of intermediate storeys is obtained by linear interpolation. Table V shows the yield strength assumed for the piles. The yield strength for the tension, compression, and bending moment is constant at any portion for all buildings. The yield strength assumed for the soil deposits is given in Table VI.

5. RESULTS

5.1. Input earthquake motions

Figure 5 shows the synthesized accelerograms and their Fourier spectra for the hypothetical $M = 8{\cdot}1$ Guerrero earthquake at the depth of 102 m. Sixty seconds of strong motions are used because the duration of the main motion is roughly 40 s. The maximum amplitude is about 30 gals, and there are predominant periods at 1·5 and 3·0 s. Since the features of the two horizontal components are quite similar to each other

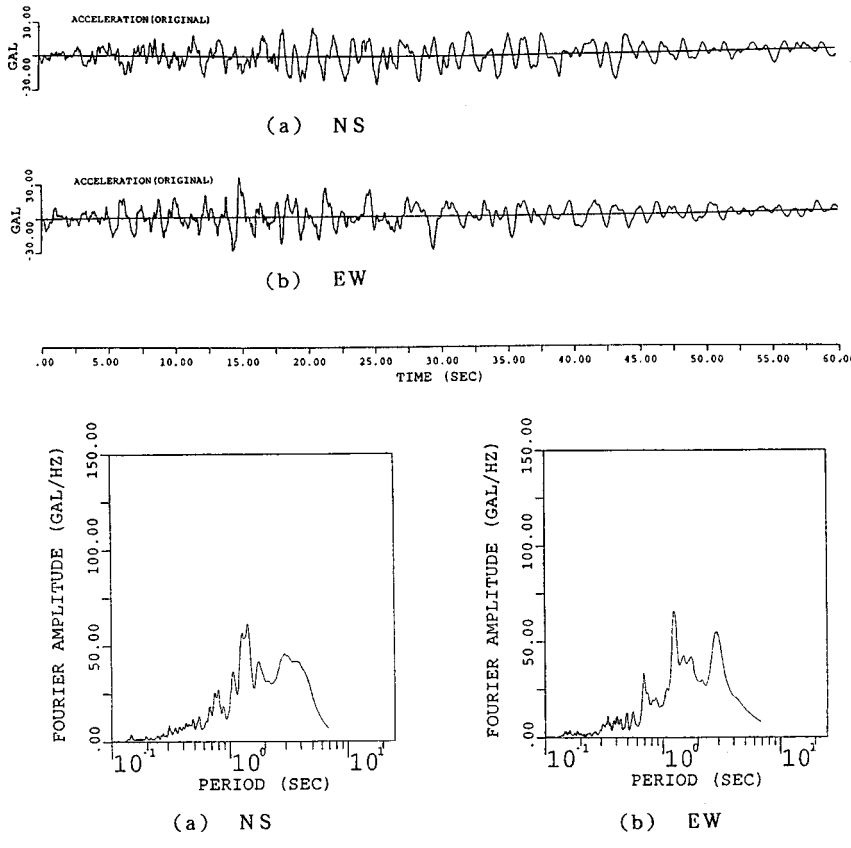

Figure 5. Synthesized accelerograms (two horizontal components) and their Fourier spectra

and the building models are symmetrical about both the directions, we will show results for only the north–south component in the following.

5.2. *Seismic-motion amplification*

Figure 6 shows the accelerograms and their Fourier spectra calculated for the linear shallow soil deposits. The predominant periods of motion on and near the ground surface are about 2·5 s, which match well with the primary predominant period calculated from the underground profile. Seismic motions are greatly amplified in the upper 10 m.

Figure 7 shows the accelerograms and their Fourier spectra calculated for the non-linear soil deposits. They are basically similar to those for the linear soil deposits. The amplitude is slightly smaller than that for the linear case and the predominant periods of motion, which are not so sharp as those for the linear case, are 2·0–2·5 s.

5.3. *Comparison of four types of analyses*

The results of the four types of analyses are compared in the case of the 15-storey building. We choose the 15-storey building, because mid-rise (7–15-storey) buildings sustained heavy damage during the 1985 earthquake, and because they experienced large soil–building interaction effects.

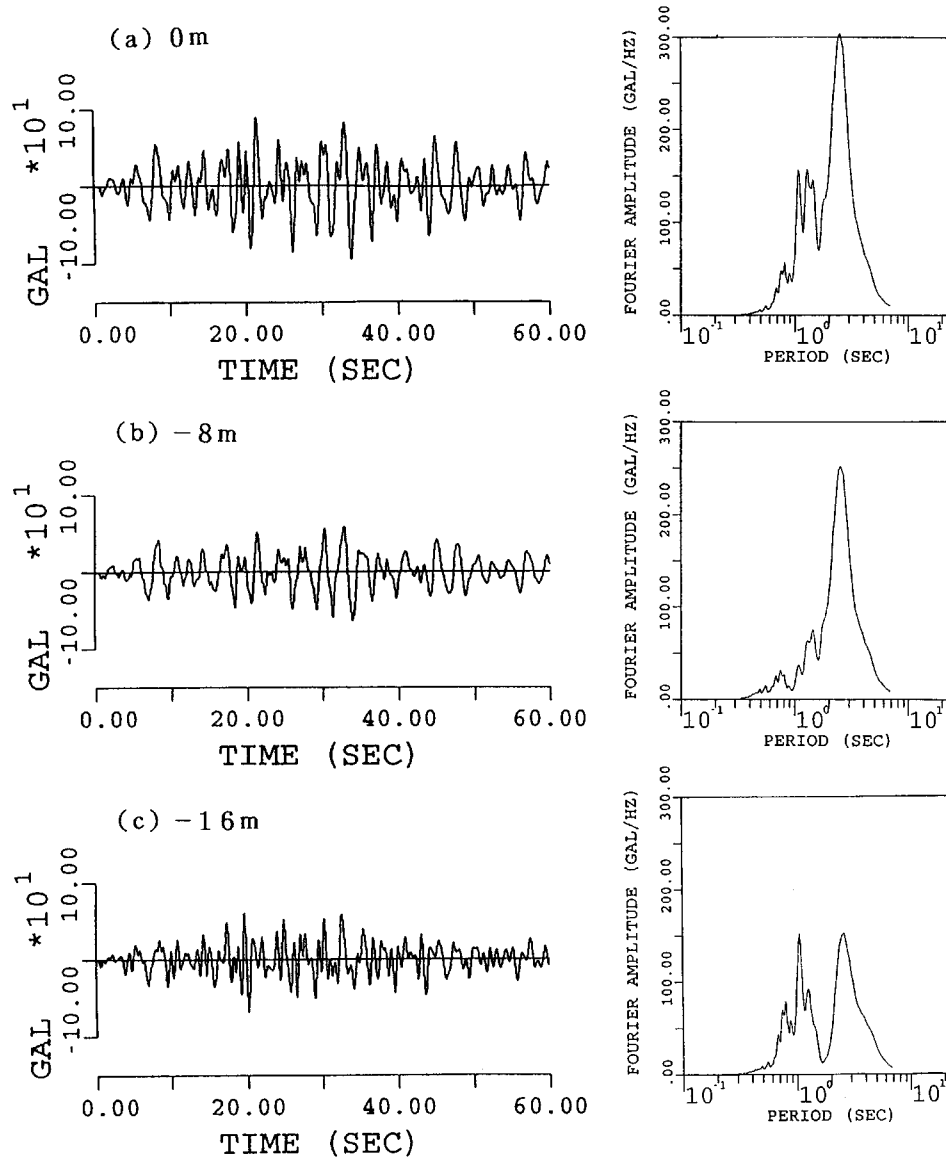

Figure 6. Free-field accelerograms (north–south component) and their Fourier spectra calculated for the linear shallow soil deposits

Top-storey accelerograms and their Fourier spectra (for the five buildings) for three types of analyses are shown in Figure 8. In all the analyses for the 15-storey building, the building superstructure behaves linearly. Since no differences are seen between the linear and non-linear cases of the base-fixed analyses, the results of the non-linear case are not shown. Owing to interaction effects, the acceleration amplitudes become smaller, and the effective fundamental period of the building becomes longer. Of the two interaction analyses, the amplitude for the non-linear case is smaller than for the linear case.

The maximum pile stresses and strains for the two interaction analyses are summarized in Table VII. Note the large contrast in the bending moment between the linear and non-linear analyses. Although this result

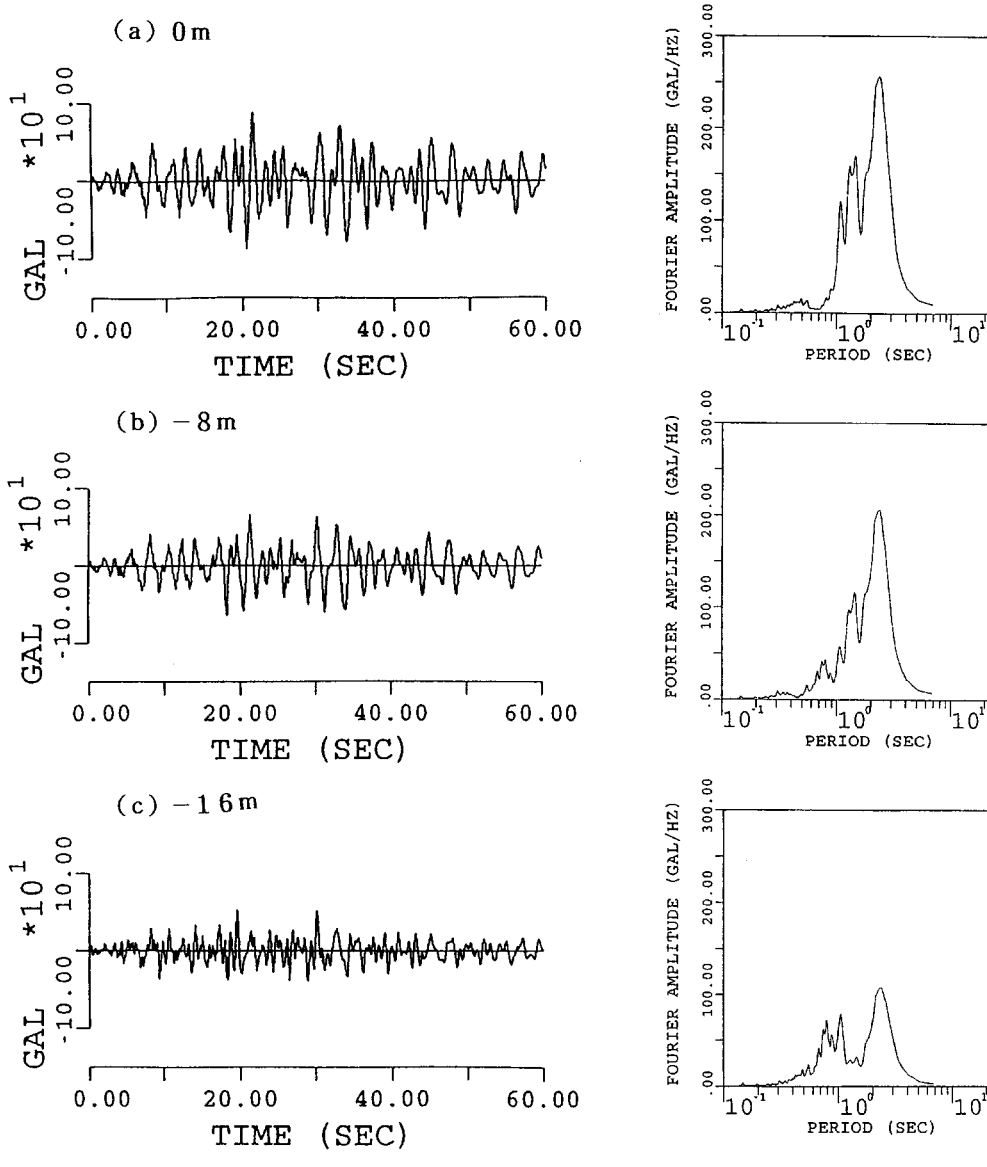

Figure 7. Free-field accelerograms (north–south component) and their Fourier spectra calculated for the nonlinear shallow soil deposits

depends on the assumed non-linear stress–strain relation of piles, the linear analysis does not provide a satisfactory result. In the lakebed zone, the high-strength surface clay is very compressible. The results of a static non-linear interaction analysis under the action of gravity are also shown in Table VII. Note that the static values of pile stresses and strains, and foundation settlement contribute fairly to the total (dynamic plus static) values.

In the non-linear interaction analysis, the superstructure behaves completely linearly. In contrast, large non-linearity of the pile responses is observed (Figure 9). If the linear analysis is employed, the bending moment becomes extremely large while the bending strain is the same as that for the non-linear analysis. The

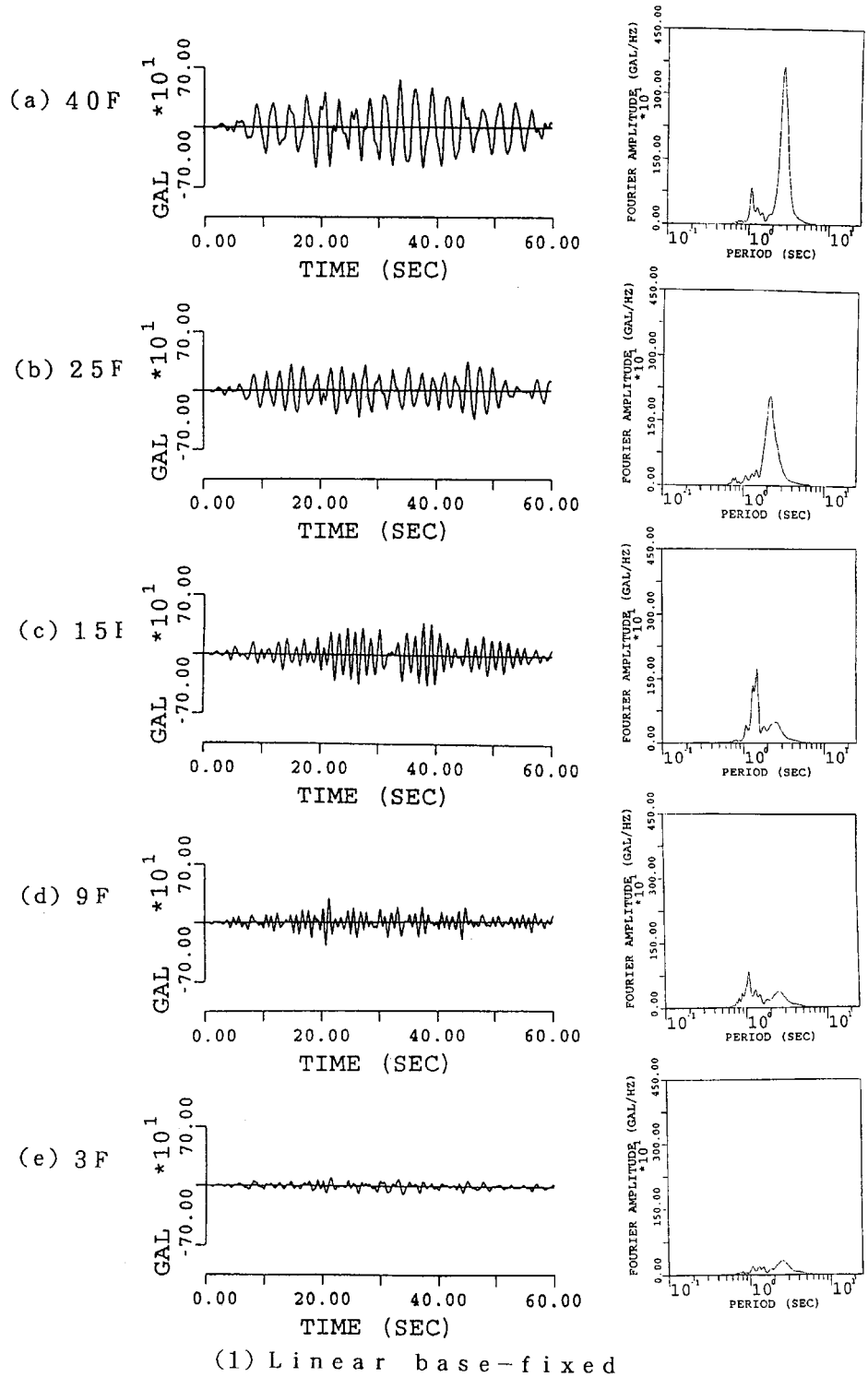

Figure 8. Top-storey accelerograms (north–south component) and their Fourier spectra for the five buildings for three types of analyses: (1) linear base-fixed analysis, (2) linear interaction analysis, and (3) non-linear interaction analysis

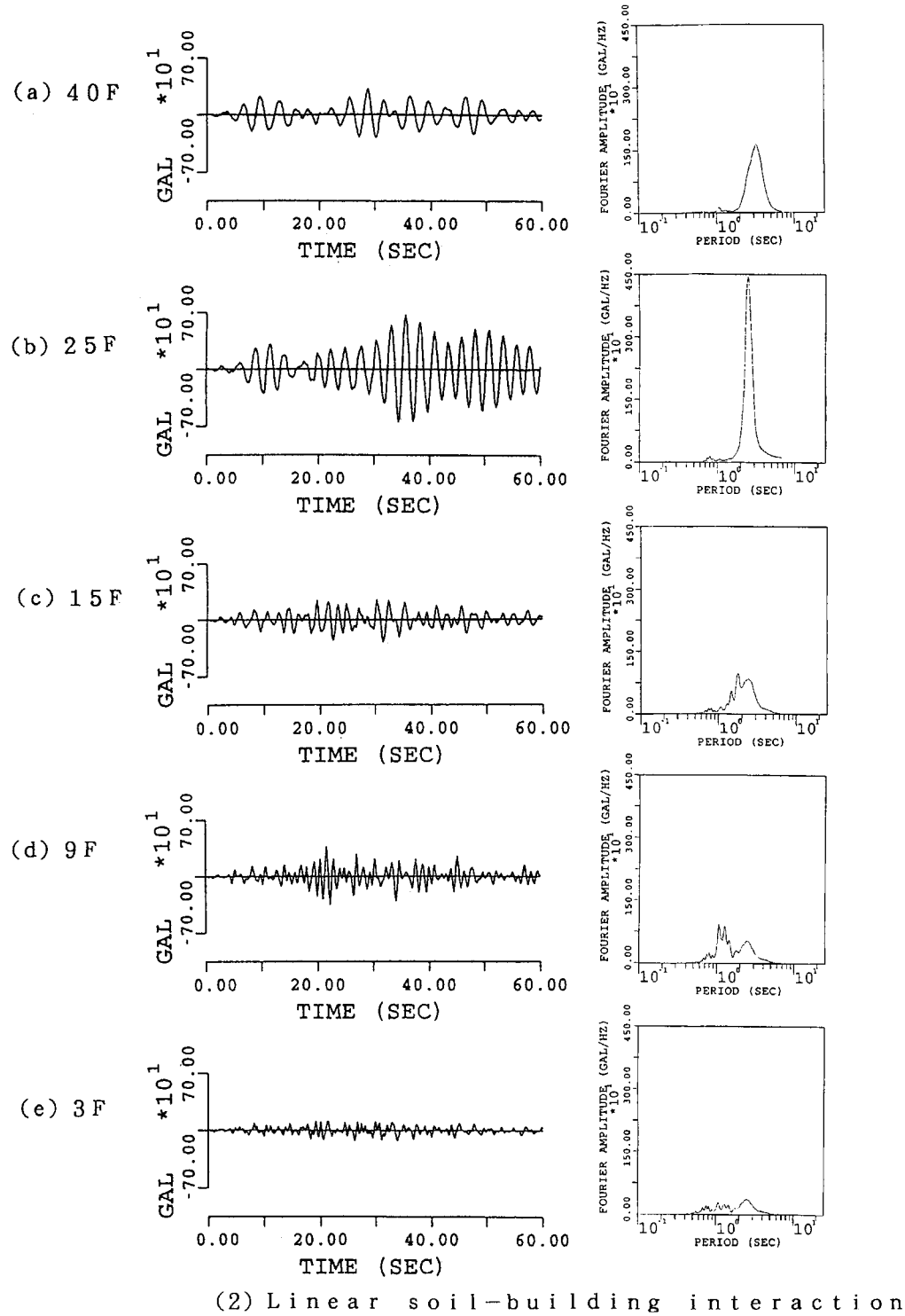

Figure 8. *Continued*

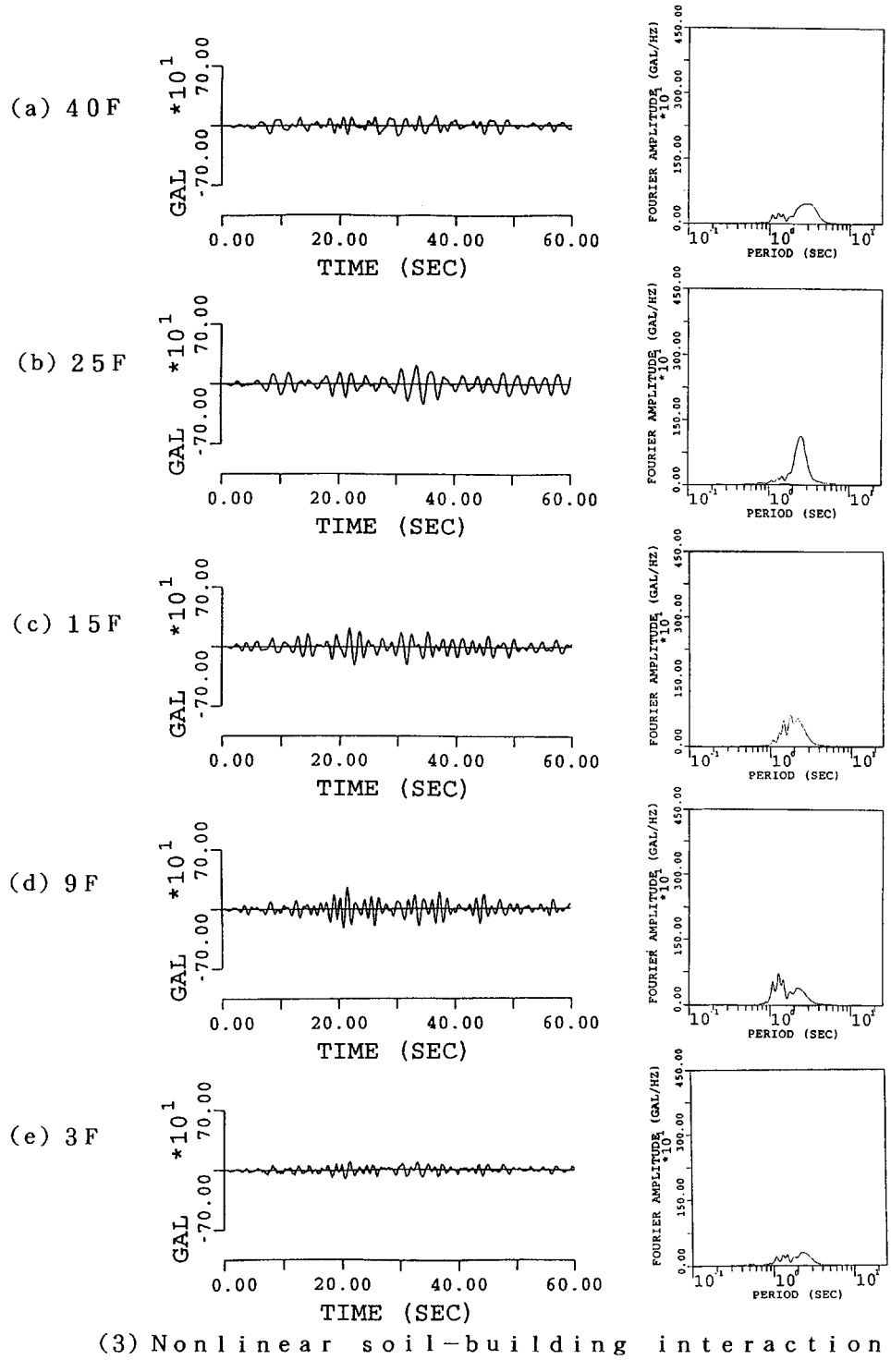

Figure 8. *Continued*

Table VII. Maximum pile stresses and strains, and foundation settlement due to ground subsidence in the 15-storey building model

	Soil-building interaction		Static load
	Linear	Non-linear	Non-linear
Axial force (t)	990	710	398
Shear force (t)	350	300	39
Bending moment (t m)	1960	80	44
Axial strain	$1{\cdot}3\times10^{-4}$	$6{\cdot}8\times10^{-5}$	$5{\cdot}2\times10^{-5}$
Shear strain	$1{\cdot}3\times10^{-4}$	$1{\cdot}1\times10^{-4}$	$1{\cdot}4\times10^{-5}$
Bending strain	$7{\cdot}1\times10^{-4}$	$7{\cdot}0\times10^{-4}$	$4{\cdot}1\times10^{-5}$
Foundation settlement (cm)	—	—	15·8

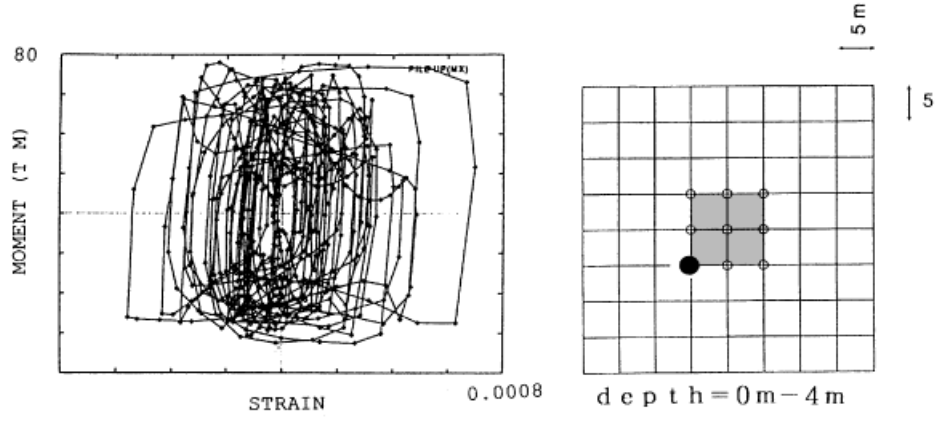

Figure 9. Stress–strain time history (north–south component) of the bending moment at the shallowest corner beam element

soil deposits behave basically linearly, and soil non-linearity is recognized only in a small volume just below the building.

5.4. *Response of the building models*

Figure 8 shows top-storey accelerograms and their Fourier spectra for the five buildings for three types of analyses (except for the non-linear base-fixed analysis). Generally, the effective fundamental periods of buildings with interaction are longer than those in the base-fixed analyses, suggesting soil–building interaction effects. The 3-storey building vibrates with a period of 2·5 s which is not the fundamental period of the building but the predominant period of the ground surface.

In the base-fixed analyses, taller buildings have higher acceleration amplitudes, and except for the 40-storey building, the building superstructure behaves linearly.

Two remarkable characteristics are seen in the linear interaction analysis. First, the response of the 25-storey building becomes excessively large, whereas the response of the 40-storey building decreases, compared to the base-fixed analyses. In contrast to a moderate building amplification due to the assumed damping (2%) in the base-fixed analyses, the 25-storey building heavily resonates with a period of 2·5 s, which is equal to the predominant period of the ground surface. This occurs because the effective fundamental

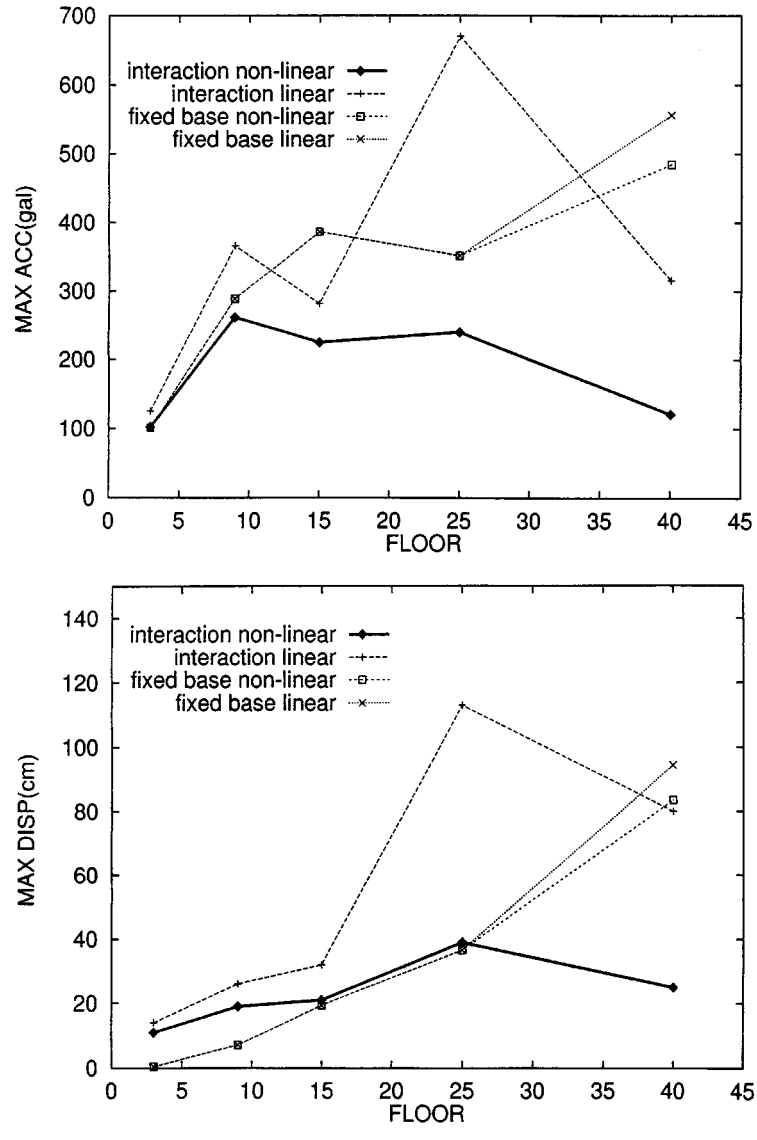

Figure 10. Relationships between the top-storey maximum acceleration and displacement (north–south component) and the number of storeys for the five buildings for the four types of analyses

period of the building with interaction becomes a little longer than the original fundamental period of the building (2·04 s). Secondly, there is an increase in the response of the 9-storey building with respect to that of a rigid base and buildings of this kind suffered heavy damage during the 1985 Michoacan earthquake.

In the non-linear interaction analysis, the 25-storey building does not resonate and the response greatly decreases. The response of the 40-storey building considerably decreases. The response of the 9-storey building is the largest although the accelerations do not reach 300 gals.

Figure 10 (upper) shows the relationship between the top-storey maximum acceleration and the number of storeys for the four types of analyses. This figure shows that there are big differences in the building responses among the analytical methods.

The results of the non-linear interaction analysis seem to be consistent with the damage pattern during the 1985 earthquake, in that the response accelerations of the 9-storey building are the largest, implying heavy damage in mid-rise buildings during the 1985 earthquake. As the 3-storey building vibrates with a period of 2·5 s, the effective fundamental period of the 9-storey building is the shortest among the five buildings.

6. DISCUSSION

The calculated building response is impacted significantly by the assumptions made in the different analytical methods. The base-fixed analyses are not able to explain the building damage pattern observed in the 1985 Michoacan earthquake, even though the surface strong motions are reasonably estimated. Interaction effects such as deamplification and prolonged effective fundamental periods of building responses can be seen in the lakebed zone of Mexico City. The linear interaction analysis provides only a partial explanation of the observed damage, and it is not satisfactory. The 25-storey building resonates heavily since the prolonged fundamental period of the building matches the predominant period of the ground surface. The linear analysis is not able to include the energy dissipation and decreasing resonance due to the inelastic behaviour of piles and soil deposits. Hence, the linear response is in practically all cases larger than the corresponding non-linear response. Finally, the non-linear interaction analysis matches relatively the observed damage pattern even though the superstructure remains linear. This means that not only interaction effects but also material non-linear effects must be considered, particularly for high-rise buildings whose fundamental periods are close to the predominant periods of ground surface in the lakebed zone.

In some cases, the soil–building interaction leads to an increase in the response with respect to that of a rigid base, while in other cases there is a decrease. This behaviour can be directly related to the particular shape of the Fourier spectra of surface motions. Soil–building interaction results in increased response with respect to the corresponding rigid-based system on ascending portions of the spectra, as the effective fundamental period of the building increases with the building-foundation coupling. The converse is true on descending branches. This means that the frequency contents of surface motions have a significant impact on the building response. It is essential that the input earthquake motions are correctly estimated.

In the previous section, building response has been discussed in terms of only the top-storey acceleration because it is the most frequently used parameter to understand building response. It is clear that displacement is a more effective parameter for understanding damage. Figure 10 (lower) shows the relationship between the top-storey maximum displacement and the number of storeys. Again, this figure underscores the big differences in the building response using different analytical methods. The maximum displacements are quite similar regardless of the building height in the non-linear interaction analysis, whereas they increase very much with building height in the other analyses.

The storey drift and shear force are considered to be more meaningful quantities for characterizing the building damage. Table VIII summarizes maximum values of the storey drifts and the ratios of the shear force to the yield strength across all storeys in the non-linear interaction analysis. These values for the 3-storey building are small, which is very consistent with the results of the top-storey acceleration. Judging from the vertical distributions of storey drifts and shear force for the 15-storey building, building collapse is likely to occur in the low stories if the assumed yield shear strength is much lower.

The amplitude of our synthetic surface motions at the Roma-C station is reasonable, judging from the comparison of our synthetics with the accelerograms recorded during the 1985 earthquake. However, probably the shear strength of the structural elements was significantly lower than the values used in our analysis, although no strong-motion records were obtained on buildings at that time. With the exception of the 40-storey building in the base-fixed analyses, the building superstructure behaves linearly, in spite of the observed heavy damage to the superstructure during the 1985 earthquake. The superstructure suffered most damage, although in some cases accompanied by foundation settlement. The foundation settlement perhaps

Table VIII. Maximum values of the storey drifts (D) and the ratios of the shear force to the yield strength (R) across all storeys for the building models

	D (cm)		R (%)	
	NS	EW	NS	EW
(1) 3-storey building	0·24	0·29	11·8	14·4
(2) 9-storey building	0·97	1·04	48·3	51·5
(3) 15-storey building	0·93	0·85	46·5	42·6
(4) 25-storey building	0·84	0·81	41·8	40·3
(5) 40-storey building	0·62	0·81	31·1	40·9

corresponds to the large pile stresses due not only to ground subsidence but also to ground shaking. This is a crucial problem that needs to be carefully investigated in our model hereafter.

Another problem to be examined is the adequacy of inputting seismic motions on the bottom plane of the model volume (the treatment as body waves). According to a cross-correlation analysis by Iida *et al.*,[15] which was done for strong-motion records obtained at the Tlacotal borehole station in the lakebed zone, body waves were dominant in the short-period range of less than 1·5 s, while surface waves were identified in the long-period range of more than 3·0 s. The wave-type identification was insufficient in the intermediate range. Judging from this result and the fundamental periods of the five building models, the degree of confidence in the response analyses for the 25-storey and 40-storey buildings, particularly for the 40-storey building is most likely not as high as desired.

7. CONCLUSIONS

The 1985 Michoacan earthquake ($M = 8{\cdot}1$) caused very severe damage to mid-rise buildings in the lakebed zone of Mexico City, which is approximately 400 km from the epicentre in the Pacific Ocean. In the present study, a 3-D non-linear soil–building interaction analysis for several types of low- to high-rise buildings during the hypothetical Guerrero earthquake was performed in order to understand the real cause of heavy damage to mid-rise buildings in the lakebed zone during the 1985 Michoacan earthquake. A reasonable estimation of the input earthquake motions and the local site effects was made.

The base-fixed analyses have not been able to explain the building damage pattern in Mexico City during the 1985 earthquake. The linear soil–building interaction analysis has provided only a partial explanation of the damage pattern, and it is not satisfactory. The results of the non-linear interaction analysis seem to be the most consistent with the observed damage pattern.

ACKNOWLEDGEMENTS

Mr. Yoshinori Furumoto at the Research and Development Center, Sumitomo Heavy Industries, Ltd. has worked with the post-processing of calculations. We thank Dr. Tetsuya Ishihara at the Technical Research and Development Institute, JDC Cooperation, Dr. Hitoshi Taniguchi at the Center for Regional Development, United Nations, and the staffs at the Research and Development Center, Sumitomo Heavy Indusries, Ltd. and at the National Disaster Prevention Center of Mexico for their sincere help. We also appreciate the support provided by the Japan International Cooperation Agency (JICA) and the JICA Mexico project committee. Research funds were provided by the Ministry of Education, Japan and the Kajima Foundation's Research Grant. Suggestions made by the journal editor and two anonymous reviewers have greatly improved this manuscript.

REFERENCES

1. H. Kobayashi, 'Relationships among microtremor, ground motion and damage distribution', *Reports on the Damage Investigation of the 1985 Mexico Earthquake by Architectural Institute of Japan*, 1987, pp. 144–156 (in Japanese).
2. J. G. Anderson, P. Bonin, J. N. Brune, J. Prince, S. K. Singh, R. Quaas and M. Onate, 'Strong ground motion from the Michoacan, Mexico, Earthquake', *Science* **233**, 1043–1049 (1986).
3. M. P. Romo, 'Clay behavior, ground response and soil–structure interaction studies in Mexico City', *Proc. 3rd Int. Conf. Recent Advances Geotechnical Engineering Soil Dynamics*, 1995, pp. 25–42.
4. T. Ishihara and F. Miura, 'Nonlinear seismic response analysis method for 3-D soil-structure interaction systems', *Proc. Japan Soc. Civil Engng* **465** (I-23), 145–154 (1993) (in Japanese).
5. K. Toki and C. S. Fu, 'Generalized method for nonlinear seismic response analysis of a three-dimensional soil-structure interaction system', *Earthquake Engng. Struct. Dyn.* **15**, 945–961 (1987).
6. K. Tamano, 'Seismic response analysis method for 3-D soil–structure interaction systems, considering soil nonlinearity', *Master's Thesis*, Yamaguchi University, 1987.
7. Y. Ohshima and H. Watanabe, 'An elasto-plastic dynamic response analysis of underground structure-soil composite based upon the 3-D finite element method', *Proc. Japan Soc. Civil Engng* **495** (I–28), 31–42 (1994).
8. S. H. Hartzell, 'Earthquake aftershocks as Green's functions', *Geophys. Res. Lett.* **5**, 1–4 (1978).
9. H. Kanamori, 'A semi-empirical approach to prediction of long-period ground motions from great earthquakes', *Bull. Seism. Soc. Am.* **69**, 1645–1670 (1979).
10. D. M. Hadley and D. V. Helmberger, 'Simulation of strong ground motions', *Bull. Seism. Soc. Am.* **70**, 617–630 (1980).
11. K. Irikura, 'Semi-empirical estimation of strong motions during large earthquakes', *Bull. Disas. Prev. Res. Inst., Kyoto University* **33**, 63–104 (1983).
12. K. Imagawa, N. Mikami and T. Mikumo, 'Analytical and semi-empirical synthesis of near-field seismic waveforms for investigating the rupture mechanism of major earthquakes', *J. Phys. Earth* **32**, 317–338 (1984).
13. M. Iida and M. Hakuno, 'Study on complexity of large earthquakes', *Proc. Japan Soc. Civil Engng* **350** (I-2), 47–57 (1984).
14. S. K. Singh, J. Lermo, T. Dominguez, M. Ordaz, J. M. Espinosa, E. Mena and R. Quaas, 'The Mexico earthquake of 19 September, 1985 — a study of amplification of seismic waves in the Valley of Mexico with respect to a hill zone site', *Earthquake Spectra* **4**, 653–673 (1988).
15. M. Iida, M. Ordaz, H. Taniguchi, C. Gutierrez and M. Santoyo, 'Interpretation of wave field inside the Mexico Valley on the basis of borehole data', *Proc. 9th Japan Earthquake Engineering Symposium*, Vol. 3, 1994, pp. E121–E126.

